AIMS Mathematics, 10(12): 29686–29702.
DOI: 10.3934/math.20251305
Received: 19 August 2025
Revised: 13 November 2025
Accepted: 20 November 2025
Published: 17 December 2025

https://www.aimspress.com/journal/Math

Research article

Padmakar-Ivan index of power graphs with applications in silicon structures

Manju S. C[1], Sakander Hayat[2,*], K. Somasundaram[3] and Rashad Ismail[4]

[1] Department of Science and Humanities, Sree Narayana Gurukulam College of Engineering, Kolenchery, Kerala, India

[2] Mathematical Sciences, Faculty of Science, Universiti Brunei Darussalam, Jln Tungku Link, Gadong BE1410, Brunei Darussalam

[3] Department of Mathematics, Amrita School of Physical Sciences, Coimbatore, Amrita Vishwa Vidyapeetham, India

[4] Department of Mathematics, Faculty of Science and Arts, Mahayl Assir, King Khalid University, Abha 61913, Saudi Arabia

* **Correspondence:** Email: sakander1566@gmail.com.

Abstract: In this study, we focus on the Padmakar-Ivan (PI) index, a molecular descriptor that quantifies the structural characteristics of chemical networks on the basis of their vertex distances. The main objective of this work is to develop efficient approaches for computing the PI index, particularly for graph powers and complex network structures. We begin by formulating an algorithm for computing the PI index of general graphs and extend it to the k^{th} power of a graph using a distance-based framework. Furthermore, we introduce a novel clique cut method that establishes a theoretical foundation for analyzing and computing the PI index in intricate silicate and silicon-based frameworks. The proposed techniques significantly simplify and generalize existing computational procedures.

Keywords: graph indices; Padmakar-Ivan index; power of a graph
Mathematics Subject Classification: 05C09, 05C35, 05C92

1. Introduction

In this article, we focus exclusively on simple connected graphs, emphasizing their significance in the realm of chemistry, particularly in the representation of chemical structures. Graph theory plays a crucial role in theoretical chemistry, where molecular structure descriptors, commonly referred to as topological indices, are employed to depict various characteristics of chemical compounds. These indices encompass physical, chemical, pharmacological, toxicological, biological, and other properties [1].

A topological index, essentially a real number associated with a graph, serves as a structural invariant. Over time, numerous topological indices have been introduced, and several of them have been utilized for modeling the various properties of chemical, pharmaceutical, and other molecular substances. The application of topological indices in the field of chemistry can be traced back to 1947, marked by the introduction of the Wiener index by the chemist Harold Wiener. Wiener utilized this index to explore the physical properties of a class of alkanes referred to as paraffins [2].

The Padmakar-Ivan (PI) index of a graph was first introduced by Padmakar Khadikar and colleagues in 2000 [3], and its applications in the field of chemistry were further investigated in subsequent studies [4]. In 2008, Khalifeh and others expanded upon this index by defining its vertex version, which involves equidistant vertices of an edge [5]. The PI index for a graph G is defined as follows:

$$PI(G) = \sum_{e=(x,y)\in E(G)} \Big(n_x(e) + n_y(e)\Big).$$

In this context, $n_x(e)$ denotes the number of vertices in the graph G that have a distance to the vertex x that is strictly shorter than their distance to the vertex y.

To enhance the variety of bipartite graphs, in [6], the authors introduced the weighted PI index. It is given by

$$PI_w(G) = \sum_{e=(x,y)\in E(G)} [d_G(x) + d_G(y)]\Big(n_x(e) + n_y(e)\Big),$$

where $d_G(x)$ is the degree of vertex x. Numerous studies have been conducted to establish bounds for topological indices, highlighting the importance of developing algorithms for exploring sets of these indices.

The computation of the PI index has been explored across various categories of molecular graphs in [7, 8]. In-depth discussions on determining the extremal values and characterizing the extremal graphs are extensively covered in [9]. The weighted PI index, applied to product graphs, has been computed as detailed in [10].

Remarkably, the investigations conducted by Manju and Somasundaram in [11] offer precise values for the PI and weighted PI indices within powers of some classes of graphs. Their work, detailed in [12], provides the determination of the PI index for bicyclic graphs, alongside an exploration of various classes of perfect graphs, as presented in [13]. More recently, they introduced a new method for computing the vertex PI index in [14], with applications to special classes of graphs, demonstrating improved computational efficiency and broader applicability.

In [15], the authors established the bounds on the Wiener index of the k^{th} power of a graph G, while in [16], the authors obtained the bounds on the hyper-Wiener index of the k^{th} power of a graph G. Ivan Gutman and his co-authors conducted a study on the Harary index for the same graph in [17].

Building upon these insights, this paper first introduces an algorithm for calculating the PI index of a graph. The algorithms proposed in Section 2 provide a straightforward method for computing the PI index of the k^{th} power of a graph.

Among various topological indices, the PI index has been widely used to analyze different chemical networks; however, existing methods for its computation often become complex when applied to networks with overlapping cliques or repeated structural units.

Despite several studies on silicate networks, the computation of the PI index for such structures remains challenging due to their repetitive tetrahedral connectivity and the difficulty in identifying

equidistant vertices. To address this gap, Section 3 introduces a new method for computing the PI index based on the contribution of cliques, offering a simpler and more general approach. This method is then applied to silicate networks to demonstrate its computational efficiency and chemical significance.

2. Algorithm for the PI index of graphs

Here, we introduce a computational algorithm for determining the PI index of a graph. For an edge e, equidistant vertices denote the vertices that share the same shortest distance to the end vertices of e. The count of such vertices of an edge e is represented as $N_G(e)$. $n_x(e) + n_y(e) = |V(G)| - N_G(e)$.

Consequently, the PI index of a graph can be calculated as

$$PI(G) = \sum_{e \in E(G)} [|V(G)| - N_G(e)] .$$

Let G be a graph with $x_1, x_2, \ldots, x_n$ as the vertices. D, the distance matrix for the graph G, is an $n \times n$ symmetric matrix, denoted as $[d_{ij}]$, $d_{ij} = d(x_i, x_j)$, represents the shortest distance between the vertices x_i and x_j in the graph G.

Algorithm 1 PI index of a graph

```
Input: Distance matrix D = [d_ij] of a graph G of order n.
Output: PI index of G.
PI(G) = 0
m = 0
Γ = 0
for i = 1 to n do
    for j = i + 1 to n do
        γ_ij = 0
        if d_ij == 1 then
            m = m + 1
            for r = 1 to n do
                if d_ir == d_jr then
                    γ_ij = γ_ij + 1
                end if
            end for
            Γ = Γ + γ_ij
        end if
    end for
end for
PI(G) = n * m − Γ
```

In this context, we introduce Algorithm 1, which is designed to calculate the PI index of a graph by utilizing the distance matrix of that graph as its input. The key objective in calculating the PI index is to identify the number of equidistant vertices associated with each edge. To achieve this, when dealing with an edge e connecting the vertices x_i and x_j, we examine the two rows in the distance matrix that

correspond to these vertices. Our approach involves tallying the number of matching positions within these rows, and we denote it by γ_{ij}, a concept that forms the foundation of the ensuing algorithm's development.

2.1. Computing the PI index for the power of a graph

The k^{th} power G^k of a graph G is a distinct graph with an identical set of vertices. In G^k, two vertices are joined by an edge if the distance between them in the original graph G is at most k. An illustrative example is provided in Figure 1.

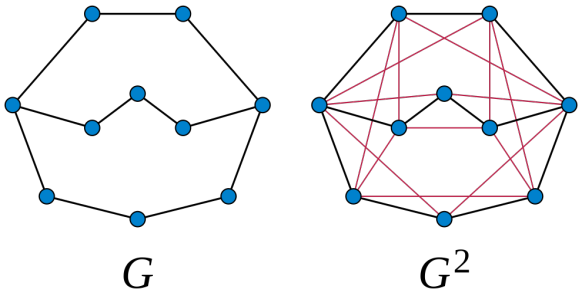

Figure 1. Second power of a graph.

In this section, we present a procedure for computing the distance matrix of the power of a graph G. Leveraging the algorithm designed for the PI index, we can then compute the PI index of the k^{th} power of the graph. Although obtaining D^k from D is straightforward, we provide a concise pseudocode to ensure reproducibility of the computational procedure (see Algorithm 2).

Algorithm 2 Distance matrix of k^{th} power of a graph G.

Input: Distance matrix $D = [d_{ij}]$ of G
Output: Distance matrix $D^k = [d^k_{ij}]$ of G^k
for $i = 1$ to n **do**
    for $j = 1$ to n **do**
        if $i = j$ **then**
            $d^k_{ij} \leftarrow 0$
        else if $d_{ij} \leq k$ **then**
            $d^k_{ij} \leftarrow 1$
        else
            $d^k_{ij} \leftarrow \lceil \frac{d_{ij}}{k} \rceil$
        end if
    end for
end for
return D^k

Example 2.1. Consider the third power of a graph P_8.

The entries in $D = [d_{ij}]$ represent the shortest distances between the vertices of P_8. Input the following:

$$D = \begin{bmatrix} 0 & 1 & 2 & 3 & 4 & 5 & 6 & 7 \\ 1 & 0 & 1 & 2 & 3 & 4 & 5 & 6 \\ 2 & 1 & 0 & 1 & 2 & 3 & 4 & 5 \\ 3 & 2 & 1 & 0 & 1 & 2 & 3 & 4 \\ 4 & 3 & 2 & 1 & 0 & 1 & 2 & 3 \\ 5 & 4 & 3 & 2 & 1 & 0 & 1 & 2 \\ 6 & 5 & 4 & 3 & 2 & 1 & 0 & 1 \\ 7 & 6 & 5 & 4 & 3 & 2 & 1 & 0 \end{bmatrix}.$$

From Algorithm 2, we obtain the distance matrix of P_8^3,

$$D^3 = \begin{bmatrix} 0 & 1 & 1 & 1 & 2 & 2 & 2 & 3 \\ 1 & 0 & 1 & 1 & 1 & 2 & 2 & 2 \\ 1 & 1 & 0 & 1 & 1 & 1 & 2 & 2 \\ 1 & 1 & 1 & 0 & 1 & 1 & 1 & 2 \\ 2 & 1 & 1 & 1 & 0 & 1 & 1 & 1 \\ 2 & 2 & 1 & 1 & 1 & 0 & 1 & 1 \\ 2 & 2 & 2 & 1 & 1 & 1 & 0 & 1 \\ 3 & 2 & 2 & 2 & 1 & 1 & 1 & 0 \end{bmatrix}.$$

In Algorithm 1, for $i = 1$ and $j = 2$, we have $d_{ij} = 1$, $m = 1$, and $\gamma_{12} = 4$. By proceeding similarly for all pairs of vertices, we finally obtain

$$PI(G) = 8 \times 18 - 62 = 144 - 62 = 82.$$

Through the application of Algorithm 2, the computation of various other topological indices for the k^{th} power of graphs becomes feasible. This methodology allows for the precise determination of indices such as the Wiener index, hyper-Wiener index, Harary index, and Sombor index for the power of a graph (for the definitions and additional details of these indices, the readers may refer to [1, 2, 15, 16, 18–20]).

We recall that an edge $e = (x, y)$ of a graph G is said to be an equidistant edge for a vertex $u \in V(G)$ if $d(u, x) = d(u, y)$. Edge e is at a distance r for a vertex u means that $d(u, x) = d(u, y) = r$. The set of all equidistant edges of u is $D_G(u) = \{e = (x, y) \in E(G) : d(u, x) = d(u, y)\}, N_G(u) = |D_G(u)|$. It is easy to see that $\sum_{e \in E(G)} N_G(e) = \sum_{u \in V(G)} N_G(u)$.

Lemma 2.1. *[13] Let G be a graph with n vertices and m edges. Then $PI(G) = mn - \sum_{u \in V(G)} N_G(u)$.*

Suppose that K_λ is a clique with λ vertices in G. Label the vertices of this clique as $v_1, v_2, \ldots, v_\lambda$. For any vertex u in G that is not part of K_λ, the distance from u to the clique K_λ is defined as $d(K_\lambda, u) = \min\{d(u, v_i) : v_i \in K_\lambda\}$; that is, the shortest distance from u to any vertex in the clique. This minimum distance is usually achieved by one or more vertices of the clique.

Each vertex u in $G \setminus K_\lambda$ divides the vertices of the clique K_λ into two sets, X and Y, according to their distances from u (see Figure 2). Specifically, the following hold.

- X consists of the vertices in K_λ that are at the minimum distance from u, i.e., $d(X, u) = d(K_\lambda, u)$.

- Y contains the remaining vertices in K_λ, each at a distance one more than the minimum, i.e., $d(Y, u) = d(K_\lambda, u) + 1$.

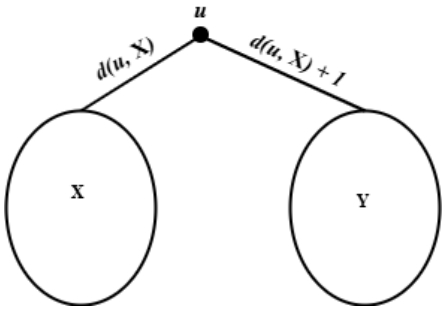

Figure 2. Representation of vertex u partitioned into sets X and Y.

This partition has an important implication.

The vertex u is equidistant to all edges within K_λ whose endpoints are both in X or both in Y.

However, u is not equidistant to the edges which have one end in X and the other end in Y.

$$N_{K_\lambda}(u) = \frac{|X|(|X|-1)}{2} + \frac{(\lambda - |X|)(\lambda - |X| - 1)}{2} = \frac{\lambda(\lambda-1)}{2} - |X|(\lambda - |X|). \tag{2.1}$$

Now, $|X| = j$ can take values from $j \in \{1, 2, ..., \lambda - 1\}$. Here, $j \neq \lambda$, since if $j = \lambda$, the clique would have a size $\lambda + 1$, which is not possible.

Let Γ_j denote the vertices in $G \setminus K_\lambda$ for which the minimum distance to the clique K_λ is attained with exactly j vertices of K_λ and $|\Gamma_j| = \gamma_j$, as seen in Figure 3.

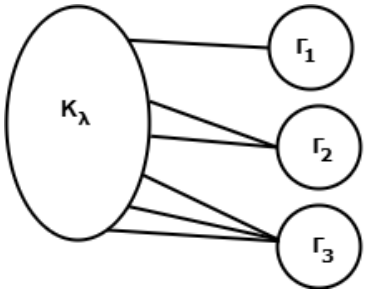

Figure 3. Illustration of the sets Γ_j relative to the clique K_λ.

Before presenting the main result in Section 3, we establish the following theorem, which shows how the clique K_λ contributes to the PI index of a graph G. This theorem also forms a key step in proving the main result for silicate networks, where cliques serve as the fundamental structural units.

Theorem 2.1. *Let K_λ be a clique in a graph G with n vertices; we then have* $\sum_{e \in K_\lambda} (|V(G)| - N_G(e)) = \lambda(\lambda-1) + \sum_{j=1}^{\lambda-1} \gamma_j j(\lambda - j)$.

Proof. Let v denote the vertex of the clique K_λ (there are λ such vertices) and $u \in G \setminus K_\lambda$; there are $n - \lambda$ such vertices outside the clique. Then, from Eq (2.1), $N_{K_\lambda}(u) = \frac{\lambda(\lambda-1)}{2} - |X|(\lambda - |X|)$, $N_{K_\lambda}(v) = \frac{(\lambda-1)(\lambda-2)}{2}$.

Now, by Lemma 2.1,

$$\begin{aligned}
\sum_{e\in E(K_\lambda)} N_G(e) &= \sum_{a\in V(G)} N_{E(K_\lambda)}(a)\\
&= \sum_{v\in K_\lambda} N_{E(K_\lambda)}(v) + \sum_{u\in G\setminus K_\lambda} N_{E(K_\lambda)}(u)\\
&= \frac{\lambda(\lambda-1)(\lambda-2)}{2} + \left(\frac{\lambda(\lambda-1)}{2}\right)(n-\lambda) - \sum_{j=1}^{\lambda-1} j\gamma_j(\lambda-j)\\
&= \frac{\lambda(\lambda-1)(\lambda-2)}{2} + \frac{\lambda(\lambda-1)(n-\lambda)}{2} - \sum_{j=1}^{\lambda-1} j\gamma_j(\lambda-j)\\
&= \frac{\lambda(\lambda-1)}{2}((\lambda-2)+(n-\lambda)) - \sum_{j=1}^{\lambda-1} j\gamma_j(\lambda-j)\\
&= \frac{\lambda(\lambda-1)}{2}(n-2) - \sum_{j=1}^{\lambda-1} j\gamma_j(\lambda-j).
\end{aligned}$$

Therefore,

$$\begin{aligned}
\sum_{e\in E(K_k)} (|V(G)| - N_G(e)) &= \sum_{e\in E(K_k)} |V(G)| - \sum_{e\in E(K_k)} N_G(e))\\
&= \sum_{e\in E(K_k)} n - \frac{\lambda(\lambda-1)}{2}(n-2) + \sum_{j=1}^{\lambda-1} j\gamma_j(\lambda-j))\\
&= n\frac{\lambda(\lambda-1)}{2} - \frac{\lambda(\lambda-1)}{2}(n-2) + \sum_{j=1}^{\lambda-1} j\gamma_j(\lambda-j)\\
&= \frac{\lambda(\lambda-1)}{2}(n-n+2) + \sum_{j=1}^{\lambda-1} j\gamma_j(\lambda-j)\\
&= \lambda(\lambda-1) + \sum_{j=1}^{\lambda-1} j\gamma_j(\lambda-j).
\end{aligned}$$

We can reduce Theorem 2.1 for K_4 as follows:

$$\sum_{e\in K_4}(|V(G)| - N_G(e)) = 12 + \sum_{j=1}^{3} j\gamma_j(4-j). \tag{2.2}$$

This quantity is referred to as the contribution of the clique K_4 to the PI index of the original graph and is denoted by $PI(K_4)_G$.

3. Silicon networks

Silicates are the fundamental building blocks of common rock-forming minerals and represent the largest, most complex, and intriguing group of minerals. Silicates are formed by fusing metal oxides or

metal carbonates with sand, and nearly all silicates contain SiO_4. A silicate sheet consists of a ring of tetrahedra connected by shared oxygen vertices, forming a two-dimensional structure where the silicon atoms are the vertices and bonds are represented as edges in a graphical model. A SiO_4 tetrahedron is illustrated in Figure 4. A silicate network of dimension n, denoted as SL_n, represents a network where n is the number of hexagons between the center and the boundary of the structure. The number of vertices in SL_n is $15n^2 + 3n$, and the number of edges is $36n^2$.

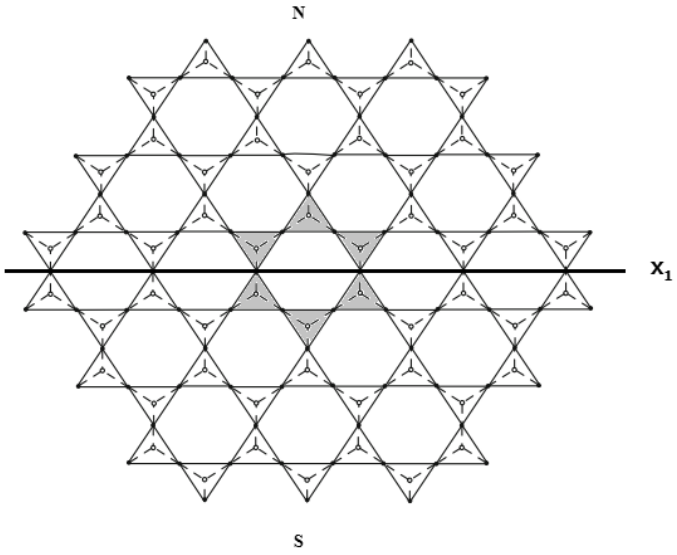

Figure 4. Silicate network of dimension 3.

The basic unit of silicates is the SiO_4 tetrahedron, which is a complete graph K_4.

Our goal is to compute the PI index of an n-dimensional silicate network using Theorem 2.1. We will achieve this by calculating the contribution of each K_4 in the graph G and then adding these individual contributions. Before we dive into the solution, there are a few important points to discuss.

3.1. Equator

Figure 4 represents Sl_3, which has three layers. The line X_1, passing through the hexagon in Layer 1, divides the entire structure into two equal halves: the upper part, denoted N, and the lower part, denoted S. We refer to the line X_1 as the equator. All the shaded tetrahedra in Figure 4 are in Layer 1.

3.2. Clique cuts

Draw lines through the oxygen nodes of the tetrahedron T (the shaded tetrahedron) as illustrated in Figure 5. These lines partition the structure into six fragments: three in the upper part, denoted N_1, N_2, and N_3, and three in the lower part, denoted S_1, S_2, and S_3. These partitioning lines are referred to as the clique cuts of the tetrahedral unit.

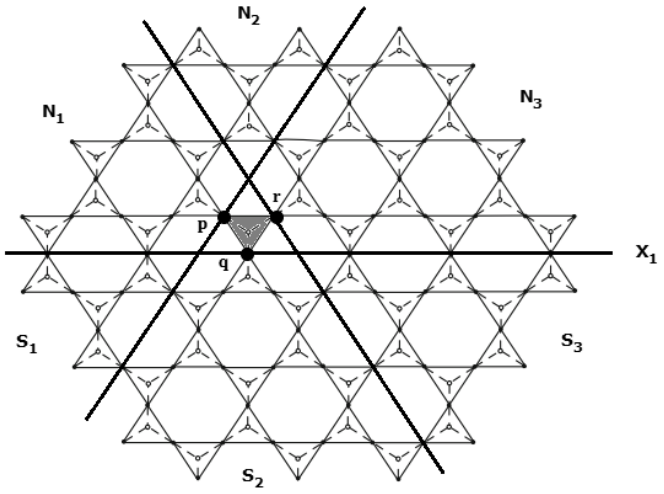

Figure 5. Clique cut.

For any vertex u within and on the boundary of the region N_1, the minimum distance to the tetrahedron $T, d(u, T)$ is always found at a specific vertex $p \in T$. Similarly, for any vertex in the region N_3 and S_2 (including its boundary), the minimum distance to T is reached at the vertices r and q, respectively. Similarly for any vertex u in the region N_2, the minimum distance to the tetrahedron $T, d(u, T)$ is always found at two vertices $p, r \in T$. In general, we can say the following.

- If the boundary of a region (potentially formed by a clique cut) includes a vertex v_T that is also in T, then the vertices within that region are closest to this common vertex v_T (among all vertices in T).
- Similarly, if a region's boundary does not share any vertex with T, then the vertices in that region are typically closest to two vertices of T.

A schematic diagram (Figure 6) has been included to visually represent the clique cut partitioning process for various values of T_r^k, which clarifies how cliques contribute to the calculation of the PI index.

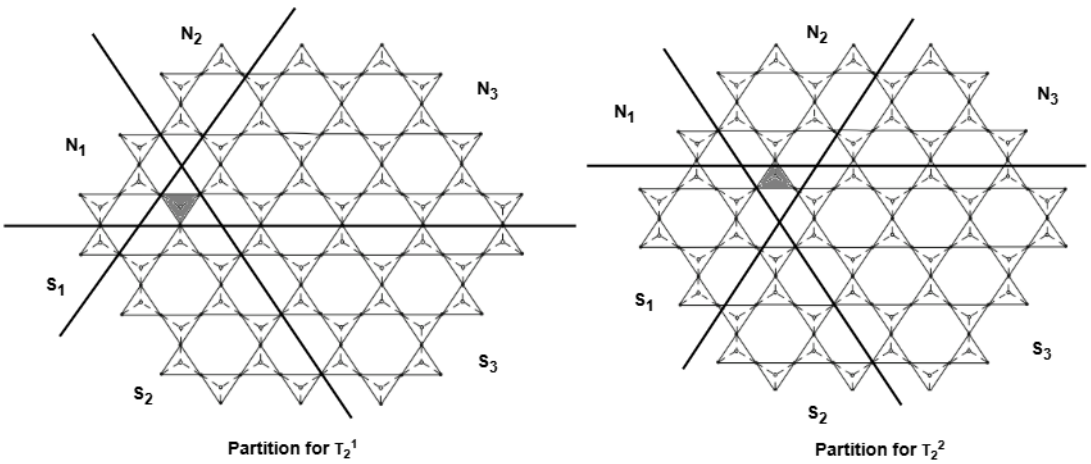

Figure 6. Schematic representation of the clique cut partitioning process for T_2^1 and T_2^2.

As in the previous section, let Γ_j denote the set of vertices in $G \setminus T$ for which the minimum distance to the clique T is reached at exactly j vertices of T. In this case, we have $\Gamma_1 = N_1 \cup N_3 \cup S_2$, $\Gamma_2 = N_2 \cup S_1 \cup S_3, \Gamma_3 = \phi$, and $\Gamma_4 = \phi$.

By Eq (2.2), we have

$$\begin{aligned} PI(K_4)_G &= \sum_{e \in K_4} (|V(G)| - N_G(e)) \\ &= 12 + \sum_{j=1}^{3} j\gamma_j(4-j) \\ &= 12 + \gamma_1(4-1) + 2\gamma_2(4-2) + 3\gamma_3(4-3) \\ &= 12 + 3\gamma_1 + 4\gamma_2 \\ &= 12 + 3(\gamma_1 + \gamma_2) + \gamma_2. \\ PI(K_4)_G &= 12 + 3(|V(G)| - 4) + \gamma_2. \end{aligned} \tag{3.1}$$

3.3. Bases of SL_n

In the structure SL_n, each layer is formed by tetrahedral units arranged symmetrically around a central hexagon. The k^{th} layer of the structure contains $12k - 6$ tetrahedral units. For example, SL_3 consists of three circular layers.

As shown in Figure 7, SL_n exhibits six lines of symmetry, dividing it into 12 equal portions. To describe the vertical position of the tetrahedra relative to the equator, we define stacks (because of symmetry, we consider only the portion on the left). Tetrahedra situated directly above the equator constitute Stack 1, with subsequent stacks placed sequentially above it. The tetrahedra in the r^{th} stack of the k^{th} layer is denoted T_r^k.

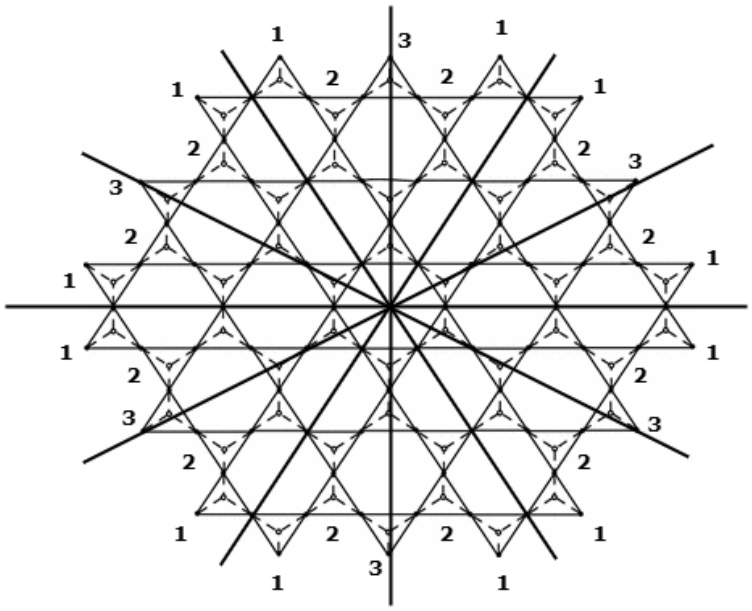

Figure 7. Lines of symmetry.

In Layer 1, there are six tetrahedra, all of which are symmetric. We designate the tetrahedron in the first layer and first stack as T_1^1. Layer 2 comprises 18 tetrahedral units. Of these, only two are non-symmetric: T_1^2, T_2^2. All other tetrahedra in Layer 2 are symmetric to either T_1^2 or T_2^2. In each layer k, there are k distinct types of tetrahedra, labeled as $T_1^k, T_2^k, \ldots, T_k^k$.

For instance, in Layer 3, there are three non-symmetric tetrahedra, marked in Figure 7 as 1, 2, and 3.

All symmetric tetrahedra contribute an equal quantity to the PI index of the graph G. We define the *bases* of SL_n as the union of all the non-symmetric tetrahedra across all layers, that is, $T_1^1, \cup_{k=1}^2 T_k^2, \cup_{k=1}^3 T_k^3, ..., \cup_{k=1}^n T_k^n$. This collection can be equivalently rearranged as $\cup_{k=2}^n T_1^k, \cup_{k=3}^n T_2^k, ..., \cup_{k=n}^n T_{n-1}^k, \cup_{r=1}^n T_r^r$. We denote this set as $\beta = \{\beta_1, \beta_2, ..., \beta_{n-1}, \beta_n\}$, $\beta_i = \cup_{k=i+1}^n T_i^k$, for $i = 1, 2, ..., n-1$, $\beta_n = \cup_{r=1}^n T_r^r$.

The bases of SL_3 are marked in Figure 8, $PI(\beta_1)_G = \sum_{e \in E(\beta_1)} (|V(G)| - N_G(e))$, $PI(SL_n) = 12 \sum_{i=1}^{n-1} PI(\beta_i) + 6PI(\beta_n)$.

Note that the choice of bases is not unique, as any non-symmetric collection of tetrahedra can serve as a base. Here, we adopt the set above as the representative base.

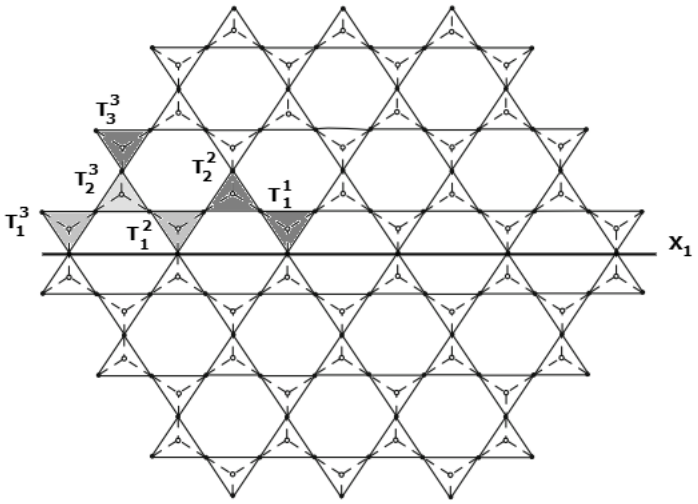

Figure 8. Bases of Sl_3.

Theorem 2.1 provides an elegant method to compute$PI(SL_n)$ using clique cuts. In this computation, we use n_r^k to denote the total number of vertices in the three fragments N_2, S_1, and S_3, corresponding to the clique T_r^k, when r is even. For an odd r, the same notation n_r^k is used to represent the total number of vertices in the fragments N_1, N_3, and S_2 associated with the clique T_r^k.

Theorem 3.1. *For a silicate network of dimension n,* $PI(SL_n) = n(315n^3 + 4n^2 + 18n - 1)$.

Proof. Let G be a silicate network SL_n.

By Eq (3.1), $PI(T_r^k) = 3(15n^2 + 3n) + n_r^k$.

The calculation proceeds by first finding n_r^k for each T_r^k.

Case 1. n is even.

Case 1.1. r is odd.

For different values of r and k, the calculated values of n_r^k are tabulated in Table 1.

Table 1. Number of vertices in different regions corresponding to $T_r^k, r \le k \le n, r \in [1, n-1]$, r is odd.

Region	Number of vertices
S_1	$\frac{n-k}{2}(4+5(n-k-1))+5\frac{(n-k)(r-1)}{2}$
S_3	$\frac{n+\frac{r-1}{2}}{2}(4+5(n+\frac{r-3}{2}))+\frac{r-1}{4}(6+10n+\frac{5(r-3)}{2})+5(n+\frac{r-1}{2})(k-r)$
N_2	$\frac{n-k}{2}(4+5(n-k-1))+5(n-k)(k-\frac{r+1}{2})$

Each entry in Tables 1 and 2 represents the number of vertices in a specific region corresponding to the tetrahedral unit T_r^k, $r \le k \le n, r \in [1, n-1]$, where r is odd. These values are computed by systematically counting the vertices in each stack and layer, taking symmetry into account. The correctness follows from the combinatorial structure of SL_n, where each layer contains $12k-6$ tetrahedra, and the network is divided into 12 symmetric portions.

$$\begin{aligned} n_r^k &= \left(\frac{n-k}{2}(4+5(n-k-1))+5\frac{(n-k)(r-1)}{2}\right) \\ &\quad +\left(\frac{n+\frac{r-1}{2}}{2}(4+5(n+\frac{r-3}{2}))+\frac{r-1}{4}(6+10n+\frac{5(r-3)}{2})+5(n+\frac{r-1}{2})(k-r)\right) \\ &\quad +\left(\frac{n-k}{2}(4+5(n-k-1))+5(n-k)(k-\frac{r+1}{2})\right) \\ &= \frac{30n^2-46n-5r^2+14k+10kr+5}{4}. \end{aligned}$$

To sum up the expression over $k, r+1 \le k \le n$

$$\begin{aligned} \sum_{k=r+1}^{n} n_r^k &= \sum_{k=r+1}^{n} \frac{30n^2-46n-5r^2+14k+10kr+5}{4} \\ &= \frac{(n-r)(30n^2-39n+12r+5rn+12)}{4}. \end{aligned}$$

We then take the sum of the expression on r, with the condition that r is an odd number between 1 and n.

$$\sum_{r\in[1,n-1],risodd}\sum_{k=r+1}^{n} n_r^k = \frac{n(95n^3-105n^2+46n+24)}{48}.$$

Moreover, $n_r^r = \frac{30n^2-46n+5r^2+14r+5}{4}$. We then take the sum of the expression on r, with the condition that r is an odd number between 1 and n.

$$\sum_{r\in[1,n-1],risodd} n_r^r = \frac{n(95n^2-117n+10)}{24}.$$

Case 1.2. r is even.

For different values of r and k, the calculated values of n_r^k are tabulated in Table 2.

$$n_r^k = \left(\frac{n-k}{2}(4+5(n-k-1))\right)+\left(\frac{n-\frac{r}{2}}{2}(4+5(n-\frac{r}{2}-1))+5(k-1)(n-\frac{r}{2})\right)$$

$$+\left(\frac{n-k+\frac{r}{2}}{2}(4+5(n-k+\frac{r}{2}-1))+5(k-1)(n-k+\frac{r}{2})\right)$$
$$= \frac{30n^2+5r^2-46n+24k-10rk}{4}.$$

Table 2. Number of vertices in different regions corresponding to T_r^k, $r \le k \le n, r \in [2,n]$, r is even.

Region	Number of vertices
N_1	$\frac{n-k}{2}(4+5(n-k-1))$
N_3	$\frac{n-\frac{r}{2}}{2}(4+5(n-\frac{r}{2}-1))+5(k-1)(n-\frac{r}{2})$
S_2	$\frac{n-k+\frac{r}{2}}{2}(4+5(n-k+\frac{r}{2}-1))+5(k-1)(n-k+\frac{r}{2})$

To sum up the expression over $k, r+1 \le k \le n$,

$$\sum_{k=r+1}^{n} n_r^k = \sum_{k=r+1}^{n} \frac{30n^2+5r^2-46n+24k-10rk}{4}$$
$$= \frac{(n-r)(30n^2-34n+7r-5rn+12)}{4}.$$

We then take the sum of the expression on r, with the condition that r is an even number between 1 and n.

$$\sum_{r\in[2,n],riseven}\sum_{k=r+1}^{n} n_r^k = \frac{5n(n-2)(17n^2-21n+10)}{48}.$$

Moreover, $n_r^r = \frac{30n^2-46n-5r^2+24r}{4}$.

We then take the sum of the expression on r, with the condition that r is an even number between 1 and n.

$$\sum_{r\in[2,n],riseven} n_r^r = \frac{n(85n^2-117n+62)}{24}.$$

We now have

$$\begin{aligned}
PI(G) &= 12\sum_{i=1}^{n-1} PI(\beta_i)_G + 6PI(\beta_n)_G \\
&= 3\times 6n^2\times(15n^2+3n) + 12\left(\frac{n(95n^3-105n^2+46n+24)}{48}\right) + 6\left(\frac{n(95n^2-117n+10)}{24}\right) \\
&\quad +12\left(\frac{5n(n-2)(17n^2-21n+10)}{48}\right) + 6\left(\frac{n(85n^2-117n+62)}{24}\right) \\
&= 3\times 6n^2(15n^2+3n) + n(45n^3-50n^2+18n-1) \\
&= n(315n^3+4n^2+18n-1).
\end{aligned}$$

Case 2. n is odd.

Case 2.1. r is odd.

$$\sum_{r\in[1,n],risodd}\sum_{k=r+1}^{n} n_r^k = \frac{(n^2-1)(95n^2-105n+36)}{48}.$$

Moreover,

$$n_r^r = \frac{30n^2-46n+5r^2+14r+5}{4}.$$

We then take the sum of the expression on r, with the condition that r is an odd number between 1 and n.

$$\sum_{r\in[1,n],risodd} n_r^r = \frac{(n+1)(95n^2-107n+36)}{24}.$$

Case 2.2. r is even.

We take the sum of the expression on r, with the condition that r is an even number between 1 and n.

$$\sum_{r\in[2,n-1],riseven}\sum_{k=r+1}^{n} n_r^k = \frac{(n-1)(85n^3-190n^2+145n-36)}{48}.$$

Moreover, $\sum_{r\in[2,n]_{riseven}} n_r^r = \frac{(n-1)(85n^2-107n+36)}{24}$.

We now have

$$\begin{aligned}
PI(G) &= 12\sum_{i=1}^{n-1} PI(\beta_i)_G + 6PI(\beta_n)_G \\
&= 3\times 6n^2\times(15n^2+3n) + 12\left(\frac{(n^2-1)(95n^2-105n+36)}{48}\right) + 6\left(\frac{(n+1)(95n^2-107n+36)}{24}\right) \\
&\quad +12\left(\frac{(n-1)(85n^3-190n^2+145n-36)}{48}\right) + 6\left(\frac{(n-1)(85n^2-107n+36)}{24}\right) \\
&= 3\times 6n^2(15n^2+3n) + n(45n^3-50n^2+18n-1) \\
&= n(315n^3+4n^2+18n-1).
\end{aligned}$$

We now illustrate the concepts used in Theorem 3.1 through the following example. Here, we find the PI index of SL_2 using the theorem above.

Example 3.1. For $n = 2$, the structure contains two layers and two stacks. The base tetrahedra are listed below.

Bases: $\{\beta_1,\beta_2\}$, where $\beta_1 = \{T_1^2\}$, $\beta_2 = \{T_1^1, T_2^2\}$.

The number of vertices in each region corresponding to each base tetrahedron is given in Table 3.

Table 3. Number of vertices in different regions corresponding to T_r^k.

T_1^1		T_1^2		T_2^2	
Region	Number of vertices	Region	Number of vertices	Region	Number of vertices
S_1	2	S_1	0	N_1	0
S_3	9	S_3	19	N_3	7
N_2	2	N_2	0	S_2	7

For T_1^1,

$$n_1^1 = 2 + 9 + 2 = 13.$$

For T_1^2,

$$n_1^2 = 0 + 19 + 0 = 19.$$

For T_2^2,

$$n_2^2 = 0 + 7 + 7 = 14.$$

We now have

$$PI(\beta_1) = 3(15 * 4 + 3 * 2) + 19 = 217,\ P(\beta_2) = 2 * 3(15 * 4 + 3 * 2) + 13 + 14 = 423,$$

$$PI(SL_2) = 12PI(\beta_1) + 6PI(\beta_1) = 5142.$$

This is given by the formula

$$PI(SL_2) = 2(315 \times 2^3 + 4 \times 2^2 + 18 \times 2 - 1) = 5142.$$

4. Conclusions

In this paper, we proposed efficient algorithms for computing the PI index of graphs. The first algorithm determines the PI index of general graphs, while the second enhances the computation of the PI index for the k^{th} power of a graph using a distance-based framework. We also introduced a novel clique cut method that provides a theoretical foundation for computing the PI index in complex structures such as silicate and silicon-based networks.

The proposed methods significantly simplify existing computational procedures and offer new structural insights into molecular networks. Beyond silicate frameworks, these approaches can be effectively applied to analyze other large-scale chemical networks and graph-based models where distance plays a key role.

The novelty of this work lies in the development of an integrated algorithmic and theoretical framework for computing the PI index, extending its applicability to higher graph powers and complex network systems. Future research may focus on optimizing these algorithms for large datasets and extending the clique cut method to other distance-based topological indices.

Author contributions

Manju S. C: Conceptualization, Methodology, Resources, Writing–original draft; K. Somasundaram: Methodology, Supervision, Validation, Writing–original draft; Sakander Hayat and Rashad Ismail: Validation, Funding acquisition, Writing final draft, Writing–review and editing. All authors have read and approved the final version of the manuscript for publication.

Use of Generative-AI tools declaration

The authors declare they have not used Artificial Intelligence (AI) tools in the creation of this article.

Acknowledgments

The authors extend their appreciation to the Deanship of Research and Graduate Studies at King Khalid University for funding this work through Large Research Project under grant number RGP2/126/46.

Conflict of interest

The authors declare no conflicts of interest.

References

1. N. Trinajstić, *Chemical graph theory*, 2 Eds., Boca Raton: CRC Press, 1992. https://doi.org/10.1201/9781315139111
2. H. Wiener, Structural determination of paraffin boiling points, *J. Am. Chem. Soc.*, **69** (1947), 17–20. https://doi.org/10.1021/ja01193a005
3. P. V. Khadikar, On a novel structural descriptor PI, *Natl. Acad. Sci. Lett.*, **23** (2000), 113–118.
4. P. V. Khadikar, S. Karmarkar, V. K. Agrawal, A novel PI index and its applications to QSPR/QSAR studies, *J. Chem. Inf. Comput. Sci.*, **41** (2001), 934–949. https://doi.org/10.1021/ci0003092
5. M. H. Khalifeh, H. Yousefi-Azari, A. R. Ashrafi, Vertex and edge PI indices of Cartesian product graphs, *Discrete Appl. Math.*, **156** (2008), 1780–1789. https://doi.org/10.1016/j.dam.2007.08.041
6. A. Ilić, N. Milosavljević, The weighted vertex PI index, *Math. Comput. Model.*, **57** (2013), 623–631. https://doi.org/10.1016/j.mcm.2012.08.001
7. A. R. Ashrafi, M. Ghorbani, M. Jalali, The vertex PI and Szeged indices of an infinite family of fullerenes, *J. Theor. Comput. Chem.*, **7** (2008), 221–231. https://doi.org/10.1142/S0219633608003757
8. P. E. John, P. V. Khadikar, J. Singh, A method of computing the PI index of benzenoid hydrocarbons using orthogonal cuts, *J. Math. Chem.*, **42** (2007), 37–45. https://doi.org/10.1007/s10910-006-9100-2
9. M. J. Nadjafi-Arani, G. H. Fath-Tabar, A. R. Ashrafi, Extremal graphs with respect to the vertex PI index, *Appl. Math. Lett.*, **22** (2009), 1838–1840. https://doi.org/10.1016/j.aml.2009.07.005
10. C. Gopika, J. Geetha, K. Somasundaram, Weighted PI index of tensor product and strong product of graphs, *Discrete Math. Algorithms Appl.*, **13** (2021), 2150019. https://doi.org/10.1142/S1793830921500191
11. S. C. Manju, J. Geetha, K. Somasundaram, PI and weighted PI indices for powers of paths, cycles, and their complements, *J. Intel. Fuzzy Syst. Appl. Eng. Tech.*, **44** (2022), 1439–1452. https://doi.org/10.3233/JIFS-221436
12. S. C. Manju, K. Somasundaram, PI index of bicyclic graphs, *Commun. Comb. Optim.*, **9** (2024), 425–436. https://doi.org/10.22049/cco.2023.27817.1360
13. M. S. Chithrabhanu, K. Somasundaram, Padmakar-Ivan index of some types of perfect graphs, *Discrete Math. Lett.*, **9** (2022), 92–99. https://doi.org/10.47443/dml.2021.s215

14. S. C. Manju, K. Somasundaram, Y. L. Shang, A new method for computing the vertex PI index with applications to special classes of graphs, *AKCE Int. J. Graphs Comb.*, **22** (2025), 117–124. https://doi.org/10.1080/09728600.2024.2424317

15. X. H. An, B. Wu, The Wiener index of the *k*th power of a graph, *Appl. Math. Lett.*, **21** (2008), 436–440. https://doi.org/10.1016/j.aml.2007.03.025

16. W. J. Zhang, B. Wu, X. H. An, The hyper-Wiener index of the *k*th power of a graph, *Discrete Math. Algorithms Appl.*, **3** (2011), 17–23. https://doi.org/10.1142/S1793830911000973

17. G. F. Su, L. M. Xiong, I. Gutman, Harary index of the *k*-th power of a graph, *Appl. Anal. Discrete Math.*, **7** (2013), 94–105.

18. K. C. Das, M. Imran, T. Vetrík, General Sombor index of graphs and trees, *J. Discrete Math. Sci. Cryptogr.*, **28** (2025), 101–111. http://dx.doi.org/10.47974/JDMSC-1918

19. S. Rouhani, M. Habibi, M. A. Mehrpouya, On Sombor index of extremal graphs, *J. Discrete Math. Appl.*, **9** (2024), 335–344. https://doi.org/10.22061/jdma.2024.11328.1101

20. J. C. Hernández, J. M. Rodríguez, O. Rosario, J. M. Sigarreta, Extremal problems on the general Sombor index of a graph, *AIMS Math.*, **7** (2022), 8330–8343. http://dx.doi.org/10.3934/math.2022464

AIMS Press